

Decay times of one-dimensional excitons in GaAs/Al_xGa_{1-x}As quantum-well wires

M. Kohl, D. Heitmann, W. W. Rühle, P. Grambow, and K. Ploog
*Max-Planck Institut für Festkörperforschung, Heisenbergstrasse 1, Postfach 800665,
 D-7000 Stuttgart 80, Federal Republic of Germany*

(Received 22 March 1990)

We have investigated the time-dependent photoluminescence (PL) of GaAs/Al_xGa_{1-x}As quantum-well wires with GaAs cross sections of 70×14 nm prepared by deep mesa etching into a quantum-well system. The decay times of the two lowest one-dimensional heavy-hole excitonic states, hh₁₁ and hh₁₂, are both about 300 ps at 5 K, which is surprisingly long and comparable to the PL lifetime of 450 ps of the heavy-hole exciton in the reference quantum-well sample. In the early-time regime, a population transfer from the hh₁₂ excitonic state to the hh₁₁ state occurs with a transfer time constant of 100 ps, which is explained by a cooling process due to acoustical-phonon scattering. Within this time, the PL is anisotropic for the different polarizations of the exciting radiation with respect to the wire direction. For larger delay times, the excitons lose their information on the polarization in the excitation beam due to the scattering processes.

One-dimensional (1D) and zero-dimensional (0D) electronic systems, in which the carriers are confined in more than one direction, have gained considerable interest in recent years. As a consequence of the additional confinement, enhanced oscillator strengths of the excitonic transitions and larger exciton binding energies are expected.¹⁻⁴ Furthermore, the peaked density of states should give rise to enhanced optical nonlinearities and higher optical gain compared to 2D and 3D structures.^{5,6} Therefore, 1D and 0D systems are promising candidates for novel optical devices, and much effort has been undertaken for their realization. However, the technological realization of such quantum wires (1D) and quantum dots (0D) has many inherent problems, e.g., GaAs-based systems produced by etching techniques often exhibit a strong nonradiative surface recombination, which limits the investigation of their optical properties. Recently, these technical difficulties have been partially overcome, and radiative transitions between 1D electron and hole subbands have been observed.⁷⁻¹² In particular, an optical anisotropy of the 1D hh and lh ground state¹⁰ [hh (lh) represents heavy hole (light hole)] and more recently also of transitions related to higher 1D hh excitonic subbands has been measured.¹² Stimulated emission in quantum wires¹¹ and enhanced exciton binding energies of 1D excitons have also been observed.¹²

We have investigated GaAs/Al_xGa_{1-x}As quantum-well wire (QWW) structures with a lateral wire width w of 70 nm by means of picosecond time-resolved photoluminescence (PL) measurements. The 2D quantum confinement gives rise to a splitting into 1D electron and hole subbands. In recent PL excitation (PLE) measurements on QWW systems we have resolved the lowest two excitonic transitions, hh₁₁ and hh₁₂.¹² The first index here denotes the quantum number in the growth direction, the second in the lateral direction. The intensities of the excitonic transitions turned out to be strongly dependent on the polarization of the exciting laser radiation with respect to the wire direction. In particular, the hh₁₂ transition was dominating the spectra for excitation with s -polarized

light, i.e., with the electric-field vector perpendicular to the plane of incidence and parallel to the wire direction.¹² Magneto-optical measurements revealed the exciton binding energies of the corresponding excitonic states, which were enhanced for the ground-state by 15% with respect to the 2D reference sample.¹² So far, no experiments on the time-dependent behavior of quantum confined quasi-1D excitons, in particular of the higher 1D subband states and the corresponding polarization dependence have been reported. The main reason has been the existence of non-radiative recombination centers often introduced by the fabrication process, which lead to a strong reduction of the effective decay-time constant, even for wire widths larger than 500 nm.¹³ Using optimized processes, we have prepared QWW systems, which reveal surprisingly long decay-time constants of the order of 300 ps. In the following, we will discuss the time-dependent PL behavior of the hh₁₁ and hh₁₂ excitonic states, in particular the polarization dependence of the corresponding time constants and compare the results with continuous-wave (cw) PL measurements.

As starting material for the wire preparation we used GaAs/Al_xGa_{1-x}As QW samples, which were grown by molecular-beam epitaxy at 560°C. They consisted of three identical QW's of 14 nm thickness, separated by 10-nm-thick Al_{0.26}Ga_{0.74}As barriers. Two 50-nm-thick Al_{0.26}Ga_{0.74}As cladding layers were grown below and above the multiple-QW region. A mask of periodic photoresist lines oriented parallel to the $\bar{1}10$ direction was prepared on top of the samples by holographic lithography. The period of the grating was about $a=250$ nm, the width of the wires w was adjusted by the development time of the photoresist to $w=70$ nm. The mask profile was later on transferred into the samples by reactive ion etching in a SiCl₄ plasma. The depth of the thus created rectangular grooves was approximately 130 nm. The wire profile was examined with a scanning electron microscope. On each QWW sample we left an unpatterned part for use as a reference. For the cw PL measurements, we excited the samples with normally incident light of a

Styryl-9 dye laser. The PL signal was analyzed by a 1-m monochromator and photon-counting techniques. The time-dependent measurements were performed with a Styryl-8 dye laser, which was synchronously pumped by a mode-locked Ar^+ laser. The pulse repetition rate was 80 MHz and the pulse width 4 ps. The PL signal was analyzed by a 0.32-m monochromator and a streak camera with a time resolution of about 10 ps. The experiments were performed in a flow cryostat at about 5 K if not otherwise indicated.

Polarization-dependent PL spectra of a QWW sample with $w=70$ nm measured under cw conditions are shown in Fig. 1. The PL intensity of the excitonic transitions is reduced by about a factor of 30 compared to the reference QW, if we take the effective area of the wires into account. This point will be discussed below in the discussion of our data. For the quiresonant excitation at 800 nm, we observe mainly the hh_{11} transition at 808.5 nm, if we excite the QWW with p -polarized light, i.e., if the electric-field vector is perpendicular to the wire direction. However, a totally different transition at 807.4 nm shows up, when we switch the polarization in the excitation beam to s polarization. A comparison with polarization-dependent PLE measurements¹² shows that for s -polarized excitation the hh_{12} transition dominates the PL spectrum. In addition, we can see in Fig. 1 that the lh_{11} transition at 804.9 nm is also optically anisotropic. It can clearly be observed for p -polarized light, however, it is nearly absent for s polarization. This anisotropy of the 1D exciton transitions is less pronounced but still observable in cw PL, if we excite the QWW nonresonantly at 750 nm, which is several LO phonon energies above the hh_{11} exciton transition. Therefore, interesting questions concerning the coupling between the hh_{11} and hh_{12} excitonic states arise, which we want to clarify in the following by time-dependent measurements.

Figure 2 shows the PL spectra of the QWW sample at 0 and 400 ps for different polarizations of the excitation light. In the corresponding reference spectrum we observe

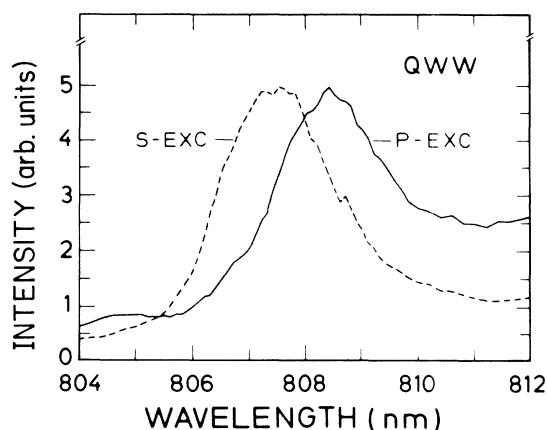


FIG. 1. cw-PL spectra of a QWW sample with a wire width of $w=70$ nm. The dashed line spectrum is observed for excitation with s -polarized laser light (S-EXC), the solid-line spectrum for p -polarized excitation (P-EXC). The excitation wavelength is 800 nm, the excitation intensity 10 mW/cm^2 .

two transitions. The first transition at 808.8 nm is due to free $e1-hh1$ excitons. This assignment is supported by intensity- and temperature-dependent PL measurements, PLE measurements, and a calculation of the transition energies with a finite potential-well model. Intensity- and temperature-dependent measurements indicate that the second line at 811 nm could be due to bound excitons. In this paper we discuss only the free-exciton transitions.

The PL spectra of the QWW sample are relatively noisy. Nevertheless, we also find the optical anisotropy stated in Fig. 1, in particular in the early time regime. At $\Delta t=0$ ps (the time window is ± 20 ps) we observe PL maxima from the lh_{11} transition and the hh_{12} transition. In the wavelength regime of the hh_{11} transition no maximum but considerable background PL is present, in particular for excitation with p -polarized light. At higher wavelengths above 809 nm, additional PL can be ob-

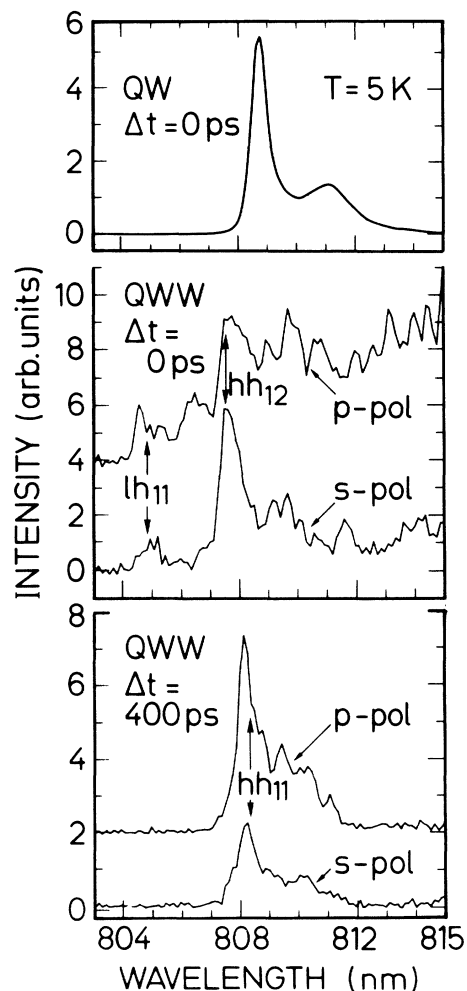


FIG. 2. PL spectra of a QWW sample with a $w=70$ nm at 0 and 400 ps together with the corresponding QW reference spectrum at 0 ps (uppermost spectrum). The time window is always 40 ps. The spectra, which are obtained for s - and p -polarization of the excitation beam, are shifted vertically with respect to each other for clarity. The scale is arbitrary but equal for the different polarizations. The excitation wavelength is 750 nm, the excitation intensity 200 W/cm^2 .

served, which is mainly due to etching-induced recombination centers. The hh_{11} transition is more pronounced in the p -polarized spectrum, while the hh_{12} transition is slightly stronger in s polarization and dominates the whole spectrum. At $\Delta t = 400$ ps the recombination of the hh_{11} transition dominates the PL spectrum in Fig. 2. The PL signal of the hh_{12} transition is now very weak, but, for s polarization, still observable as a shoulder on the shorter wavelength side of the hh_{11} transition. The intensity of the hh_{11} transition is also polarization dependent, in particular it is about a factor of 3 higher for excitation with p polarization.

We now want to discuss the time-dependent behavior of the hh_{11} and hh_{12} transition in more detail by means of Fig. 3. In the uppermost part of Fig. 3 we have plotted the time dependence of the hh_1 ground-state exciton for the reference sample. The decay is single-exponential after $\Delta t = 100$ ps, with a time constant of $\tau = 450$ ps. This result agrees well with reported values in the literature.¹⁴ The decay curves of the hh_{11} and hh_{12} transition show characteristic differences for both polarizations. Up to $\Delta t = 200$ ps, the PL intensity of the hh_{11} transition remains almost constant, while the hh_{12} transition intensi-

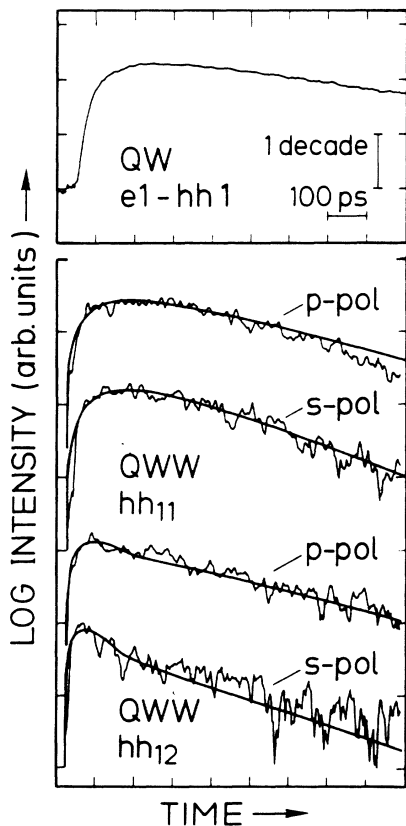


FIG. 3. Time evolution of the excitonic transitions hh_{11} and hh_{12} of a QWW sample with $w = 70$ nm together with the corresponding reference spectrum of the ground-state hh exciton (uppermost curve). For clarity, the spectra are shifted vertically with respect to each other, s -pol and p -pol denote the polarization of the excitation beam. The solid lines are fits with rate equations involving a three-level model. The excitation wavelength is 750 nm, the excitation intensity 200 W/cm^2 .

ty decreases rapidly. Obviously a population transfer from the hh_{12} excitonic state to the hh_{11} excitonic state occurs during this time period in addition to other possible decay mechanisms of both states like the radiative decay or the population transfer to etching induced states. In order to simulate the decay curves we therefore consider the following three-level model,

$$\begin{aligned} \frac{dn_p}{dt} &= -\frac{n_p}{\tau_{p \rightarrow 2}} - \frac{n_p}{\tau_{p \rightarrow 1}}, \\ \frac{dn_2}{dt} &= \frac{n_p}{\tau_{p \rightarrow 2}} - \frac{n_2}{\tau_{e2}} - \frac{n_2}{\tau_{2 \rightarrow 1}} + K \frac{n_1}{\tau_{1 \rightarrow 2}}, \\ \frac{dn_1}{dt} &= \frac{n_p}{\tau_{p \rightarrow 1}} - \frac{n_1}{\tau_{e1}} + \frac{n_2}{\tau_{2 \rightarrow 1}} - K \frac{n_1}{\tau_{1 \rightarrow 2}}. \end{aligned} \quad (1)$$

The indices 1, 2, p denote, respectively, the excitonic states hh_{11} and hh_{12} and an upper state, which is pumped by the laser. The upper excited state populates the hh_{11} (hh_{12}) state with an effective time $\tau_{p \rightarrow 1}$ ($\tau_{p \rightarrow 2}$), which includes both the relaxation and exciton formation time. The times τ_{e1} and τ_{e2} are effective decay-time constants including other possible decay mechanisms, whose importance will be discussed below, $\tau_{2 \rightarrow 1}$ describes the population transfer from the hh_{12} to the hh_{11} state. After the excitons have reached a final temperature of about 15 K the reverse process, i.e., the thermally activated transition of hh_{11} excitons into the hh_{12} excitonic state has to be taken into account. We describe this process in a simple approach by the rate $Kn_1/\tau_{1 \rightarrow 2}$ with $K=1$ for $n_1/n_2 < \exp(-\Delta E/kT)$ and $K=0$ otherwise, where ΔE is the energy difference between the two states and $\tau_{1 \rightarrow 2}$ is comparable to $\tau_{2 \rightarrow 1}$.

The time-dependent behavior of the excitonic populations $n_i(t)$, which are assumed to be proportional to the observed intensities $I_i(t)$, was obtained by numerically solving Eq. (1). In the early time regime the time-dependent behavior is given by the initial carrier population of the excited level p , $n_p(0)$, the effective relaxation times $\tau_{p \rightarrow i}$, and the population transfer time $\tau_{2 \rightarrow 1}$. The behavior for larger time delays ($\Delta t > 200$ ps) is mainly determined by the effective decay times τ_{ei} and the activation process characterized by $\tau_{1 \rightarrow 2}$. We fitted the time-dependent decay of the hh_{11} and hh_{12} transitions with the different time constants and $n_p(0)$ as fit parameters. The corresponding fit curves are plotted in Fig. 3 together with the experiment. For all four decay curves we find an effective relaxation time $\tau_{p \rightarrow i}$ of about 70 ps. This result is comparable to typical exciton-formation times in QW systems.¹⁵ For the transfer time $\tau_{2 \rightarrow 1}$ our fits consistently reveal a value of about 100 ps, which is independent of the polarization. This value corresponds roughly to an energy loss rate of $2 \times 10^7 \text{ eV/s}$. This is a typical value for energy-loss rates by acoustical deformation potential interaction at carrier temperatures below 50 K in 3D systems.¹⁶ Therefore, we interpret the exciton transfer as a cooling process due to acoustical-phonon scattering.

Since the number of scattering processes increases with decreasing excitation wavelength a decrease of the optical anisotropy in the PL is expected. By the scattering the excitons lose their information on the polarization of the excitation. On the other hand, the anisotropy of the PL in

the early regime is strong enough to cause an optical anisotropy even in the cw PL as discussed above in Fig. 1. Due to the coupling between the hh_{12} and hh_{11} states all effective decay-time constants τ_{ei} , which are determined to be about 300 ps, turn out to be independent of the polarization of the excitation light. Since the value for τ_{ei} reflects all kinds of competing decay channels of the hh_{11} and hh_{12} excitonic states, in principle, two interpretations of the data presented so far are possible.

(i) Feldmann *et al.* reported, for QW systems, that an increase of the scattering of excitons, in particular by phonons due to an increased lattice temperature, leads to an increase of the radiative decay time.¹⁷ A similar increase of scattering could also hold for our QWW systems, since etching-induced defects could lead to enhanced scattering and thus increase the radiative decay time even at low temperatures. An enhancement of scattering would therefore give rise to even longer radiative decay times than the reference decay-time constant of 450 ps. In this case the decay time $\tau_{ei} \approx 300$ ps would be dominated by nonradiative processes according to $\tau_{ei}^{-1} = \tau_r^{-1} + \tau_{nr}^{-1}$, where τ_{nr} (τ_r) is the nonradiative (radiative) decay time. Our experiments set, in any case, a lower limit of 300 ps for τ_{nr} . This value, however, is much larger than previously reported values for decay-time constants of systems, where nonradiative surface recombination was the dominant decay mechanism.¹³

(ii) Second, nonradiative processes could play a minor role in our QWW structures. In this case the observed time constants τ_{ei} mainly reflect τ_r . Hence, the observation that τ_{ei} is smaller than the radiative decay time of the hh excitons in the reference sample indicates an enhancement of the oscillator strength for the radiative recombination in the QWW. This is actually expected due to the additional quantum confinement in the lateral direction of QWW systems. However, due to the scattering between the different excitonic states, the decay times do not give any information about the anisotropy of the oscillator

strengths of the hh_{11} and hh_{12} states, which is expected from cw PL and PLE measurements.¹²

To clarify the importance of the nonradiative decay processes we measured the temperature dependence of τ_{ei} . In the case of the QW reference sample these measurements have revealed an increase of the hh excitonic decay-time constant as it is expected for dominant radiative recombination. For the QWW samples a similar but weaker tendency was observed. In particular, at $T = 30$ K τ_{ei} is approximately 1 ns. We therefore conclude that nonradiative processes play a minor role for the decay of the observed excitons in the QWW. Hence, the reduction of the PL intensity by a factor of 30, which we observe in our cw PL measurements, cannot be explained by nonradiative processes. A possible explanation of this reduction could be a change of the coupling efficiency of the excitation light into the wire system due to the different geometry of the QWW compared to the QW.

In conclusion, we have investigated the decay-time constants of the hh_{11} and hh_{12} excitonic transitions of GaAs/Al_xGa_{1-x}As QWW samples. At $T = 5$ K, the time constants are in the order of 300 ps showing a tendency to increase with increasing temperature. This indicates that radiative recombination processes are dominant in our QWW samples. The time-dependent PL intensities of the excitonic signals reveal a characteristic polarization dependence, which is consistent with cw PL measurements. In the early time regime ($t < 100$ ps) a significant transfer of hh_{12} excitons to the hh_{11} excitonic state is observed, which is explained by a cooling process due to acoustical phonon scattering. Due to the scattering processes the excitons lose their information on the polarization in the excitation for larger time delays than 100 ps.

We would like to thank M. Hauser for technical assistance with the sample growth. This work was supported by the Bundesministerium für Forschung und Technologie, Bonn, Germany.

¹J. W. Brown and H. N. Spector, Phys. Rev. B **35**, 3009 (1987).
²M. H. Degani and O. Hipolito, Phys. Rev. B **35**, 9345 (1987).
³I. Suemune and L. A. Coldren, IEEE J. Quantum Electron. **QE-24**, 1778 (1988).
⁴G. W. Bryant, Phys. Rev. B **37**, 8763 (1988).
⁵S. Schmitt-Rink, D. A. B. Miller, and D. S. Chemla, Phys. Rev. B **35**, 8113 (1987).
⁶Y. Arakawa and A. Yariv, IEEE J. Quantum Electron. **QE-22**, 1887 (1986).
⁷J. Cibert, P. M. Petroff, G. J. Dolan, S. J. Pearton, A. C. Gosard, and J. H. English, Appl. Phys. Lett. **49**, 1275 (1986).
⁸Y. Hirayama, S. Tarucha, Y. Suzuki, and H. Okamoto, Phys. Rev. B **37**, 2774 (1988).
⁹D. Gershoni, H. Temkin, G. J. Dolan, J. Dunsmuir, S. N. G. Chu, and M. B. Panish, Appl. Phys. Lett. **53**, 995 (1988).
¹⁰M. Tsuchiya, J. M. Gaines, R. H. Yan, R. J. Simes, P. O.

Holtz, L. A. Coldren, and P. M. Petroff, Phys. Rev. Lett. **62**, 466 (1989).

¹¹E. Kapon, D. M. Hwang, and R. Bhat, Phys. Rev. Lett. **63**, 430 (1989).

¹²M. Kohl, D. Heitmann, P. Grambow, and K. Ploog, Phys. Rev. Lett. **63**, 2124 (1989).

¹³G. Mayer, B. E. Maile, R. Germann, A. Forchel, and H. P. Meier, Superlatt. Microstruct. **5**, 579 (1989).

¹⁴E. O. Göbel, J. Kuhl, and R. Höger, J. Lumin. **30**, 541 (1985).

¹⁵J. Kusano, Y. Segawa, Y. Aoyagi, S. Namba, and H. Okamoto, Phys. Rev. B **40**, 1685 (1989).

¹⁶M. Pagnet, J. Collet, and A. Cornet, Solid State Commun. **38**, 531 (1981).

¹⁷J. Feldmann, G. Peter, E. O. Göbel, P. Dawson, K. Moore, C. Foxon, and R. J. Elliot, Phys. Rev. Lett. **59**, 2337 (1987).